

## SUPPLEMENTAL RESULTS

A breakdown of the patient demographics (Supplemental Table 1), injected tetrofosmin activity and acquisition-date difference between PET and SPECT studies (Supplemental Table 2) showed little difference between the ammonia and rubidium patients. The Rb82 MBF values were originally calibrated against ammonia studies and so the two tracers provide consistent estimates of myocardial blood flow. Thus, it is expected that the relation between SPECT measured K1 values and PET MBF would be consistent between PET tracers and this is what was observed (Supplemental Figure 1). For these reasons, the data from the Rb82 and ammonia patients were pooled together for the analysis presented in this work.

Global K1 values measured with different approaches to the SPECT processing (with and without attenuation correction (AC), with and without motion correction (MC), and with and without tracer-to-blood-binding corrections (BB)) are different, but can all be fit to a process-specific Renkin-Crone model for the extraction fraction function (Supplemental Figure 1). The quality of the fit, as measured by the coefficient of determination ( $R^2$ ), is improved with MC and with BB, but not with AC.

After converting K1 to MBF with the appropriate extraction fraction correction, the SPECT studies without motion correction (MC) show good correlation with PET MBF (Supplemental Figure 2), but reduced correlation compared to studies with MC (Fig. 3). Correlations between SPECT MFR and PET MFR (Supplemental Figure 2) are similarly reduced compared to images with MC (Fig. 3). The slopes of the linear fit of SPECT MBF to PET MBF are consistently better with +AC, +MC, and +BB, but the differences are not statistically significant (Supplemental Table 3). Similarly, based on the relative difference between SPECT and PET MFR, the MFR showed trends to improvement with +AC, +MC, and +BB, but the differences between correction approaches were not found to be significant (Supplemental Table 4).

## SUPPLEMENTAL DISCUSSION

We note that the majority of patients in this study were male. Gender-based differences have been seen with PET imaging (30,31) and would also be expected with SPECT, but additional studies with larger numbers of female subjects are needed to confirm this.

The myocardial flow reserve is the most commonly used metric when evaluating absolute flow measurements, but both MFR and one of rest MBF or stress MBF are needed for a complete picture of the heart's function (2). Some PET studies have also shown that stress MBF can be a useful indicator of disease (32). As a threshold for abnormal stress flow with 82Rb PET, we use 1.2 ml/min/g corresponding to two standard deviations below the mean value for normal subjects (33). Using the mean parameters from Table 1 for the Renkin-Crone model to convert stress K1 to MBF, the results are similar to those for MFR (Supplemental Table 5). There is a consistent improvement in the  $A_{ROC}$  for BB and MC. With BB and MC, there is similar  $A_{ROC}$  for detecting an abnormal PET MBF for both +AC and -AC. Using the DeLong approach to comparing the ROC curves (21), we found the AROC for +AC+MC+BB (0.965) was greater than -AC-MC-BB (0.778,  $p=0.03$ ) and +AC-MC-BB (0.859,  $p=0.04$ ); -AC+MC+BB (0.954) was greater than -AC-MC-BB (0.778,  $p=0.04$ ); +AC-MC+BB (0.940) was greater than +AC-MC-BB

(0.859,  $p=0.03$ ); and +AC+MC-BB (0.931) was greater than -AC-MC-BB (0.778,  $p=0.05$ ). ROC curves are shown for stress MBF in Supplemental Figure 3.

Data are limited on the Renkin-Crone parameters that describe the flow-dependence of the extraction fraction for tetrofosmin. The data are also difficult to compare as the extraction fraction function will depend on the corrections applied to the images during reconstruction and subsequent kinetic analysis. The 95% confidence limits of the values obtained in our study overlap (Supplemental Table 6) with those from a previous study in humans (10) and in pigs (13), but we note that the uncertainties are relatively large and this can have a substantial impact on the precision of the MBF measurements (34). Further studies to refine the parameter measurements would, therefore, be beneficial. We note that there is also an expectation that tetrofosmin would behave similarly to sestamibi. There is good agreement with the values measured in this study and those measured previously in animals (13,35) for sestamibi (Supplemental Figure 4). Despite the similarity in clinical performance between sestamibi and tetrofosmin, the results of our work cannot be extended directly to studies with sestamibi as there is not any data that we are aware of regarding confirmation of the extraction fraction function for sestamibi in humans.

Representative time-activity curves (TAC) from a stress SPECT and corresponding stress PET Rb82 study are shown in Supplemental Figure 5, along with associated polar map representations of the relative uptake and K1 or Flow distributions. The SPECT data show similar, though noisier, TAC and similar tracer distributions.

The measured myocardial TAC ( $C_{\text{myo}}(t)$ ) contains both myocardial tissue and blood contributions due to partial volume effects and the presence of blood vessels in the myocardium.

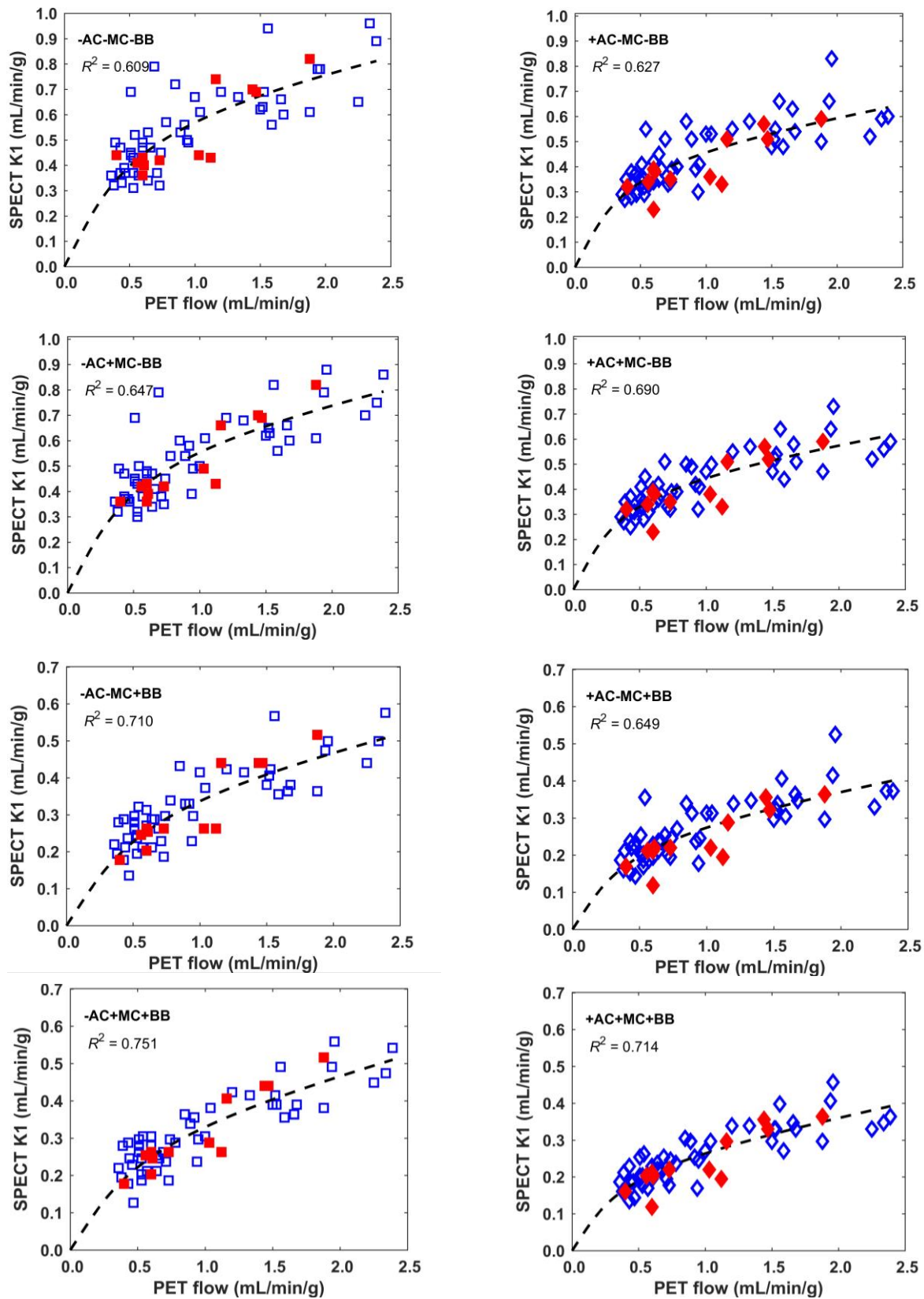
$$C_{\text{myo}}(t) = \text{FBV} C_b(t) + (1-\text{FBV}) C_t(t)$$

where  $C_b(t)$  is the blood TAC,  $C_t(t)$  is the myocardial tissue TAC, and FBV is the fractional blood volume (18). FBV is an additional parameter which is fit during the kinetic analysis. As expected, the reduced spatial resolution of SPECT compared to PET results in an increase in the mean FBV (Supplemental Table 7). The increased mixing of blood in the  $C_{\text{myo}}(t)$  signal also suggests that implementing the dual-spillover correction (18), as is done in PET, may be beneficial for SPECT MBF measurement.

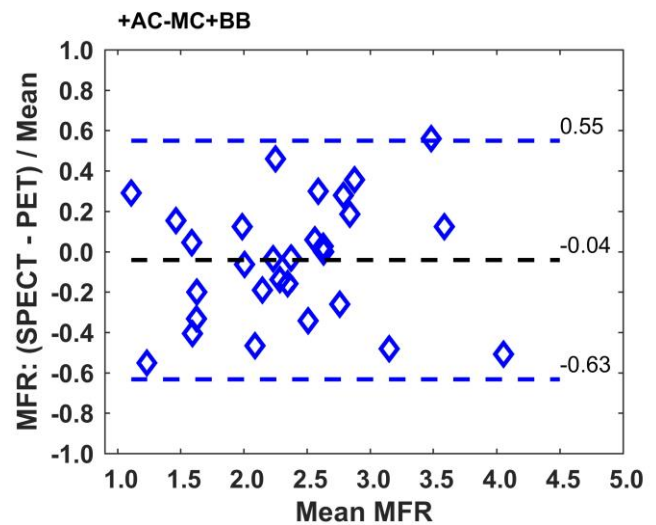
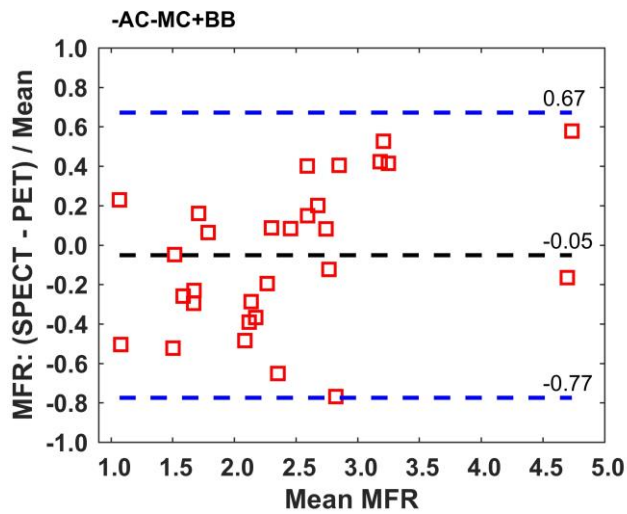
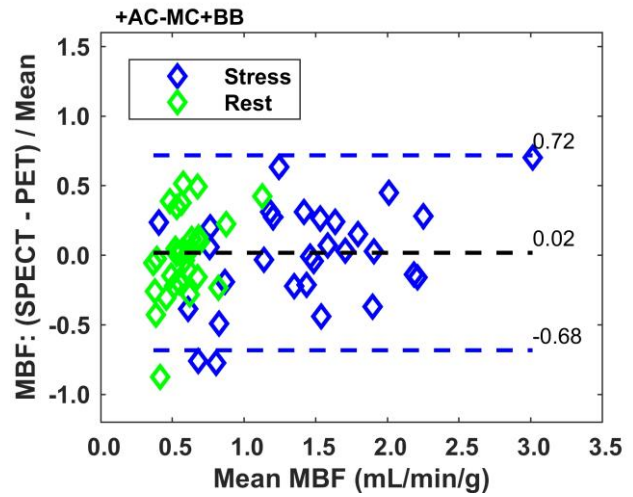
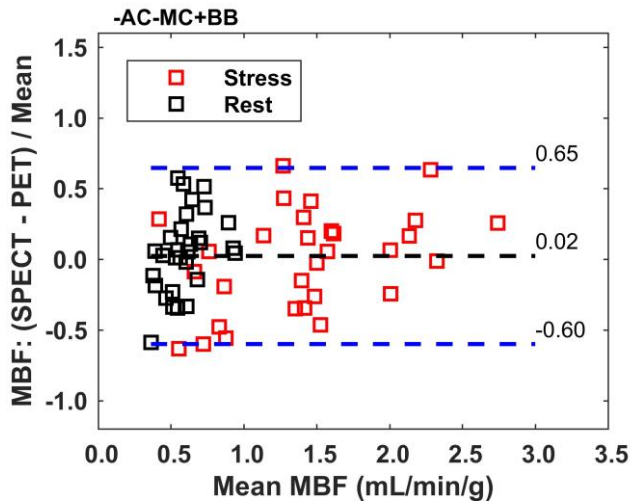
## SUPPLEMENTAL REFERENCES

30. Danad I, Raijmakers PG, Appelman YE, et al. Coronary risk factors and myocardial blood flow in patients evaluated for coronary artery disease: a quantitative [ $^{15}\text{O}$ ]H $_2\text{O}$  PET/CT study. *Eur J Nucl Med Mol Imaging*. 2012;39:102-112.
31. Duvernoy CS, Meyer C, Seifert-Klauss V, Dayanikli F, Matsunari I, Rattenhuber J, Höss C, Graeff H, Schwaiger M. Gender differences in myocardial blood flow dynamics: lipid profile and hemodynamic effects. *J Am Coll Cardiol*. 1999;33:463-470.
32. Danad I, Uusitalo V, Kero T, et al. Quantitative Assessment of Myocardial Perfusion in the Detection of Significant Coronary Artery Disease: cutoff values and diagnostic accuracy of quantitative [ $^{15}\text{O}$ ]-H $_2\text{O}$  PET imaging". *J Am Coll Cardiol*. 2014; 64:1464-1475.

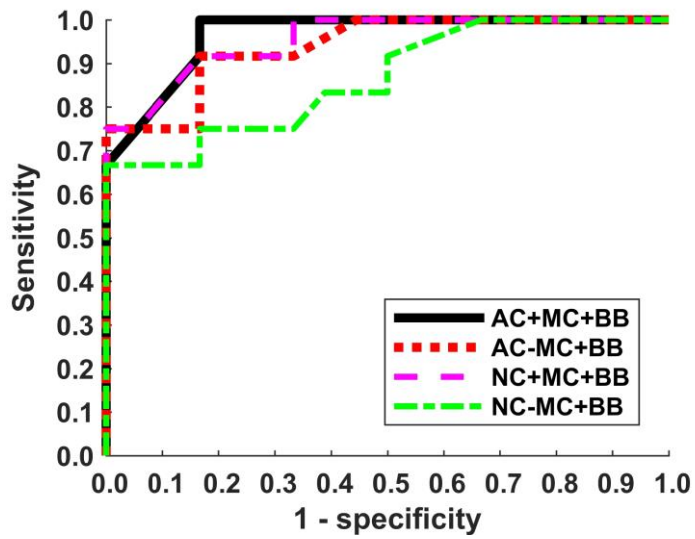
33. Lortie M, Beanlands RS, Yoshinaga K, Klein R, Dasilva JN, DeKemp RA. Quantification of myocardial blood flow with  $^{82}\text{Rb}$  dynamic PET imaging. *Eur J Nucl Med Mol Imaging*. 2007;34:1765-1774.
34. Moody JB, Murthy VL, Lee BC, Corbett JR, Ficaro EP. Variance Estimation for Myocardial Blood Flow by Dynamic PET. *IEEE Trans Med Imaging*. 2015;34:2343-2353.
35. Leppo JA, Meerdink DJ. Comparison of the myocardial uptake of a technetium-labeled isonitrile analogue and thallium. *Circ Res*. 1989;65:632-639.



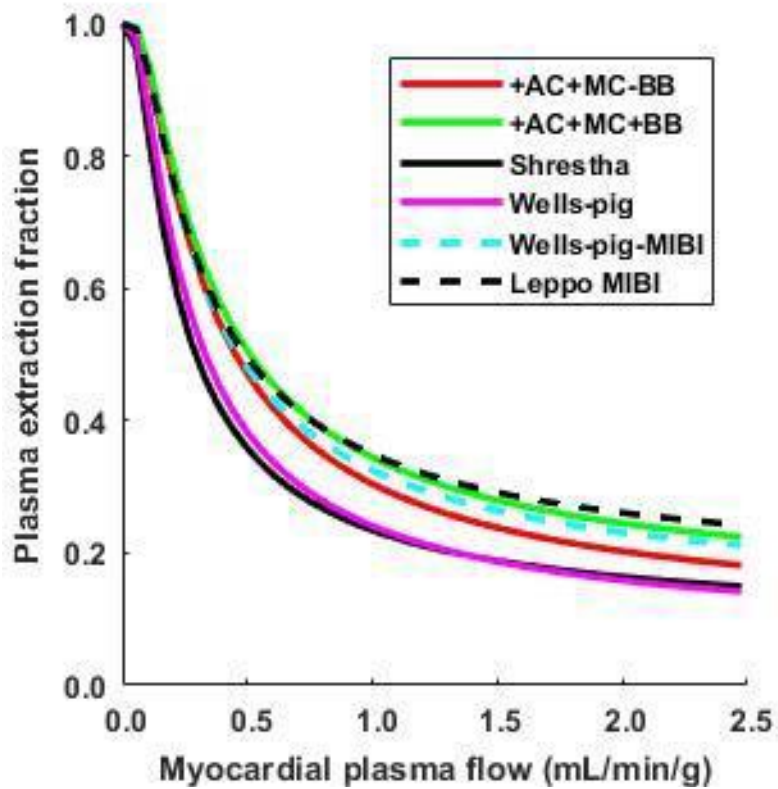
Supplemental Figure 1: Ammonia versus  $^{82}\text{Rb}$ . Scatter plots of global SPECT K1 vs PET MBF for different combinations of attenuation (AC), motion (MC), and tracer-to-blood-binding (BB) corrections show the  $^{82}\text{Rb}$  data in blue (open) and the ammonia data in red (filled). The scatter of the ammonia data generally falls within that of the  $^{82}\text{Rb}$  data and so the data were pooled for analysis. The Renkin-Crone model fit of SPECT K1 and PET flow is shown as a solid line.



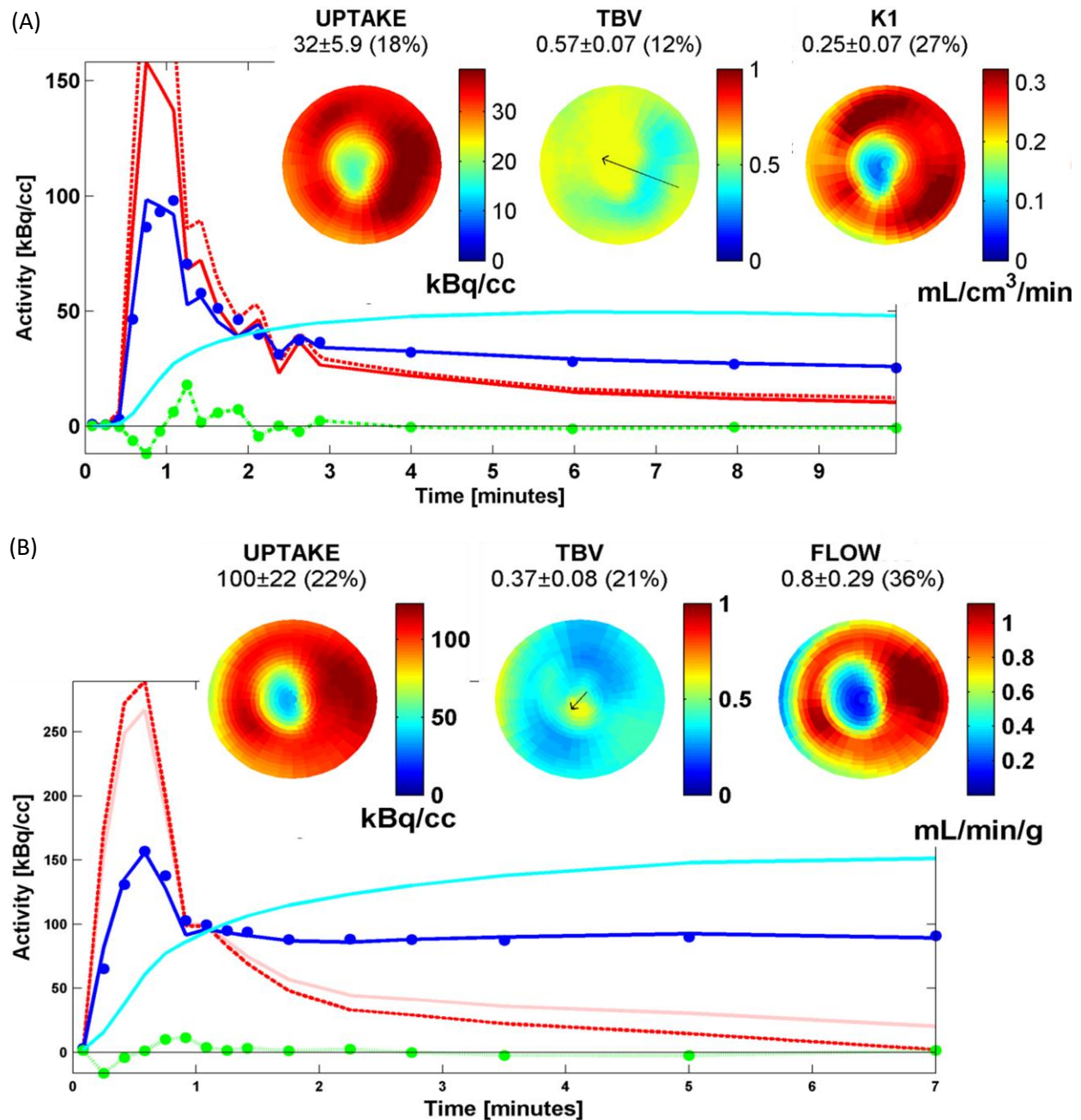
Supplemental Figure 2: Global SPECT MBF (top) and MFR (bottom) compared to PET, without (-AC) and with (+AC) attenuation correction (N=31 patients (MBF), N=29 patients (MFR)). SPECT MBF values were calculated using the mean of 50-repeat 2-fold cross-validation fit with a Renkin-Crone model for the extraction fraction. MFR is stress MBF / rest MBF. Shown are results for images without (-AC) and with (+AC) attenuation correction and without motion corrections. A blood-binding correction was incorporated in all the kinetic analyses. Dashed lines indicate mean and  $\pm 1.96$  SD.



Supplemental Figure 3: ROC curve for detecting an abnormal PET stress MBF ( $<1.2\text{ ml/min/g}$ ) using SPECT stress MBF. There were 12/30 abnormal PET stress MBF cases.



Supplemental Figure 4: Comparison of extraction fractions corresponding to the Renkin-Crone model parameters given in Supplemental Table 5, assuming a human hematocrit of 0.45. The tracer is tetrafosmin in all cases except those labeled with MIBI, which correspond to sestamibi.



Supplemental Figure 5: Example time-activity curves with associated polar maps from a stress SPECT (A) acquisition and corresponding stress PET scan (B). SPECT time-activity curves (TAC) are similar to but noisier than the PET TAC. Distribution of tracer in the uptake polar maps and also between the SPECT K1 polar map and the PET FLOW polar map. Values indicated for Uptake, fractional blood volume (TBV), K1, and Flow are the mean and standard deviation of those values over 75% of the maximum value.



Supplemental Table 1: Patient Demographics, divided by PET tracer.

	Rb82 (N=25)	NH3 (N=6)	All (N=31)
Male # (%)	22 (88)	5 (83)	27 (87)
Age (years)	65 ± 11	63 ± 12	64 ± 11
BMI (kg/m <sup>2</sup> )	25.8 ± 3.6	31.0 ± 4.7	27.9 ± 4.7
Diabetes Mellitus # (%)	5 (20)	1 (17)	6 (19)

Supplemental Table 2: Injected tetrofosmin activities and difference in acquisition dates (PET-SPECT).

	Rb82 (N=25)	NH3 (N=6)	All (N=31)
Rest (MBq)	307 ± 65	345 ± 88	316 ± 70
Stress (MBq)	1094 ± 170	1195 ± 161	1122 ± 170
Acquisition date difference (days)	20 ± 9	15 ± 10	19 ± 9
SPECT before PET # (%)	9 (36)	3 (50)	12 (39)

Supplemental Table 3: Slopes and intercepts for linear fits of SPECT MBF to PET MBF from cross-validation analysis (global) and from using the mean Renkin-Crone parameters for conversion (regional).

Correction			Global		Regional	
			Slope	Intercept	Slope	Intercept
-BB	-AC	-MC	1.19	-0.03	0.92	0.13
		+MC	1.07	0.03	0.87	0.13
	+AC	-MC	1.10	0.02	1.02	0.06
		+MC	1.06	0.02	1.06	0.02
+BB	-AC	-MC	1.09	0.00	0.92	0.09
		+MC	1.03	0.02	0.86	0.10
	+AC	-MC	1.05	0.04	0.99	0.08
		+MC	1.03	0.04	1.00	0.04

Supplemental Table 4: Comparison of SPECT and PET MFR.

Correction			SPECT MFR – PET MFR			
			Global Difference/ Mean		Regional Difference/ Mean	
			Mean	SD <sup>§</sup>	Mean	SD <sup>§</sup>
-BB	-AC	-MC	-0.03	0.47	-0.04	0.49
		+MC	-0.05	0.41	-0.05	0.43
+BB	+AC	-MC	-0.02	0.35	-0.02	0.40
		+MC	-0.01	0.32	0.01	0.37
	-AC	-MC	-0.05	0.37	-0.07	0.38
		+MC	-0.07	0.33	-0.09	0.34
+AC	-MC	-0.04	0.30	-0.05	0.34	
	+MC	-0.02	0.28	-0.02	0.31	

\* +MC vs –MC, p<0.004;

† +AC vs –AC, p<0.004;

‡ +BB vs –BB, p<0.004;

§ SD is standard deviation in the MFR difference/mean.

Supplemental Table 5: Sensitivity, specificity and area under the receiver-operating-characteristic curve (A<sub>ROC</sub>) for detecting global PET stress MBF < 1.2 with SPECT stress MBF for different corrections.

Correction			Global PET stress MBF < 1.2 (N=12/29)				
			Threshold <sup>§</sup>	Sens <sup>§</sup>	Spec <sup>§</sup>	Acc	A <sub>ROC</sub>
-BB	-AC	-MC	0.86	0.58	1.00	0.83	0.778
		+MC	1.28	0.83	0.83	0.83	0.889
+BB	+AC	-MC	1.53	0.92	0.67	0.77	0.859
		+MC	1.50	1.00	0.78	0.87	0.931
	-AC	-MC	0.95	0.67	1.00	0.87	0.866
		+MC	1.37	0.92	0.83	0.87	0.954
+AC	-MC	1.46	0.92	0.83	0.87	0.940	
	+MC	1.66	1.00	0.83	0.90	0.965	

\* +MC vs –MC for A<sub>ROC</sub>, p<0.004;

† +AC vs –AC for A<sub>ROC</sub>, p<0.004;

‡ +BB vs –BB for A<sub>ROC</sub>, p<0.004;

§ Threshold chosen to maximize Sens x Spec, using mean Renkin-Crone model parameters (Table 1);

Sens=Sensitivity, Spec=Specificity, Acc=Accuracy

Supplemental Table 6: Comparison of Renkin-Crone model parameters for the extraction fraction

Source	Species	Tracer	$\alpha$	$\alpha$ 95% CI	$\beta$ (ml/min/g)	$\beta$ 95% CI (ml/min/g)
+AC+MC-BB	human	tetrofosmin	0.090	0.039 – 0.141	0.496 <sup>¶</sup>	0.422 – 0.570
+AC+MC+BB	human	tetrofosmin	0.140	0.075 – 0.205	0.282	0.229 – 0.335
Wells*	pig	tetrofosmin	0.070	0.041 – 0.099	0.206	0.167 – 0.245
Shrestha <sup>†</sup>	human	tetrofosmin	0.091	-0.105 – 0.287	0.32	0.006 – 0.634
Wells*	pig	sestamibi	0.114	0.051 – 0.215	0.286	0.168 – 0.352
Leppo <sup>‡</sup>	rabbit	sestamibi	0.175	0.095 – 0.255	0.254	0.162 – 0.346

\* Wells et al, *J Nucl Med.* 2014. (13)

<sup>†</sup> Shrestha et al, *J Nucl Cardiol.* 2016. (10)

<sup>‡</sup> Data refit from Leppo et al, *Circ Res.* 1989. (35)

<sup>¶</sup> As the extraction fraction is a function of blood-flow, rather than plasma flow,  $\beta$  for +AC+MC-BB is equivalent to  $\beta$  for +AC+MC+BB times (1-HCT), where HCT is the human hematocrit = 0.45.

Supplemental Table 7: Average Fractional Blood Volume (FBV) measured during kinetic analysis

Method	FBV - rest	FBV - stress
PET	0.31 ± 0.06	0.32 ± 0.07
SPECT (average)	0.42 ± 0.06	0.47 ± 0.06
-AC-MC-BB	0.43 ± 0.05	0.47 ± 0.06
-AC+MC-BB	0.40 ± 0.06	0.45 ± 0.07
-AC-MC+BB	0.44 ± 0.05	0.49 ± 0.05
-AC+MC+BB	0.43 ± 0.06	0.49 ± 0.06
+AC-MC-BB	0.41 ± 0.06	0.45 ± 0.06
+AC+MC-BB	0.39 ± 0.07	0.44 ± 0.07
+AC-MC+BB	0.43 ± 0.06	0.48 ± 0.05
+AC+MC+BB	0.41 ± 0.06	0.46 ± 0.06